James Cassuto,[1] Huijuan Dou,[1] Istvan Czikora,[1] Andras Szabo,[1] Vijay S. Patel,[2] Vinayak Kamath,[2] Eric Belin de Chantemele,[3] Attila Feher,[1] Maritza J. Romero,[1] and Zsolt Bagi[1]

Peroxynitrite Disrupts Endothelial Caveolae Leading to eNOS Uncoupling and Diminished Flow-Mediated Dilation in Coronary Arterioles of Diabetic Patients

Peroxynitrite ($ONOO^-$) contributes to coronary microvascular dysfunction in diabetes mellitus (DM). We hypothesized that in DM, $ONOO^-$ interferes with the function of coronary endothelial caveolae, which plays an important role in nitric oxide (NO)-dependent vasomotor regulation. Flow-mediated dilation (FMD) of coronary arterioles was investigated in DM (n = 41) and non-DM (n = 37) patients undergoing heart surgery. NO-mediated coronary FMD was significantly reduced in DM patients, which was restored by $ONOO^-$ scavenger, iron-(III)-tetrakis(*N*-methyl-4'pyridyl)porphyrin-pentachloride, or uric acid, whereas exogenous $ONOO^-$ reduced FMD in non-DM subjects. Immunoelectron microscopy demonstrated an increased 3-nitrotyrosine formation ($ONOO^-$-specific protein nitration) in endothelial plasma membrane in DM, which colocalized with caveolin-1 (Cav-1), the key structural protein of caveolae. The membrane-localized Cav-1 was significantly reduced in DM and also in high glucose–exposed coronary endothelial cells. We also found that DM patients exhibited a decreased number of endothelial caveolae, whereas exogenous $ONOO^-$ reduced caveolae number. Correspondingly, pharmacological (methyl-β-cyclodextrin) or genetic disruption of caveolae (Cav-1 knockout mice) abolished coronary FMD, which was rescued by sepiapterin, the stable precursor of NO synthase (NOS) cofactor, tetrahydrobiopterin. Sepiapterin also restored coronary FMD in DM patients. Thus, we propose that $ONOO^-$ selectively targets and disrupts endothelial caveolae, which contributes to NOS uncoupling, and, hence, reduced NO-mediated coronary vasodilation in DM patients.

Diabetes 2014;63:1381–1393 | DOI: 10.2337/db13-0577

Diabetes mellitus (DM) is associated with impaired function of coronary resistance arteries. The consequence is a mismatch between myocardial blood supply and demand, leading to ischemic episodes in the diabetic heart (1). Reduced myocardial perfusion may develop even in the absence of occlusive coronary artery disease. For instance, Nitenberg et al. (2) have demonstrated that in DM patients with angiographically normal coronary

[1]Vascular Biology Center, Medical College of Georgia, Georgia Regents University, Augusta, GA
[2]Department of Surgery, Medical College of Georgia, Georgia Regents University, Augusta, GA
[3]Department of Physiology, Medical College of Georgia, Georgia Regents University, Augusta, GA

Corresponding author: Zsolt Bagi, zbagi@gru.edu.

Received 10 April 2013 and accepted 10 December 2013.

See accompanying article, p. 1200.

arteries, cold pressor test–induced dilation was reduced, as estimated by coronary surface area during quantitative angiography. Intracoronary injection of acetylcholine (ACh), which normally dilates arteries, caused vasospasm preferentially in diabetic patients (3). In small coronary arteries dissected from the heart of diabetic patients, Miura et al. (4) and recently our group (5) demonstrated ACh-induced constriction. The underlying mechanism(s) responsible for coronary microvascular dysfunction remained poorly understood in human DM.

Flow-mediated dilation (FMD), the intrinsic regulatory mechanism of resistance arteries in response to increases in wall shear stress (WSS) (6), is one of the key determinants of myocardial perfusion (7). The endothelium-dependent FMD is responsible for normalizing WSS and provides a feed-forward mechanism for increases in myocardial blood flow and metabolite-induced vasodilation (6). The problem is that this regulatory mechanism often fails in the diseased heart. Early studies have shown that brachial artery FMD is reduced in patients with type 1 (8) and type 2 DM (9). Previously, we demonstrated that in a mouse model of type 2 DM (*db/db* mice), WSS-induced dilation is diminished in coronary arterioles, which is due to the reduced availability of nitric oxide (NO) (10,11). In DM, among other key pathological mechanisms responsible for reduced NO synthase (NOS) activation (12,13), the direct interaction of NO with superoxide anion (14) has received substantial attention. It is of particular importance that the NO-superoxide interaction not only reduces NO bioavailability but also generates the reactive peroxynitrite ($ONOO^-$). $ONOO^-$ has numerous detrimental effects in the cardiovascular system and plays a crucial role in the development of DM-associated vascular pathology (15). Emerging evidence indicates that $ONOO^-$ preferentially targets vascular endothelium and specific subcellular compartments within (15). The footprint of enhanced $ONOO^-$ production is 3-nitrotyrosine (3-NT) formation. 3-NT–modified proteins were detected even in the normal rat aorta endothelium, with a distinct localization to mitochondria (16). Some evidence indicates that in aging rat, 3-NT formation is enhanced and more widely distributed within subcellular compartments of the endothelium (17). Yet, it is unknown whether $ONOO^-$ preferentially targets endothelial plasma membrane microdomains, such as caveolae, a specific type of cholesterol-rich membrane lipid raft, which plays a key role in WSS-induced, NO-dependent regulation of arterial diameter (18).

Accordingly, in this study, we set out to investigate alterations in coronary FMD in DM patients and to elucidate the impact of $ONOO^-$, which we hypothesized preferentially targets endothelial caveolae. In this study, we demonstrate that NO-mediated coronary FMD is markedly reduced in patients with DM. We show that $ONOO^-$ targets and disrupts endothelial membrane caveolae, which subsequently predisposes NOS for uncoupling in DM.

RESEARCH DESIGN AND METHODS

Patients

Protocols were approved by the institutional review board at our institution. Consecutive patients undergoing heart surgery were enrolled in this study. Patients were divided into two groups with or without documented DM. Patients were included irrespective of DM duration.

Assessment of FMD in Human Coronary Arterioles

Video microscopy of isolated human coronary arterioles were performed as previously described (19). In brief, coronary arterioles (diameter ~100 μm) were dissected from the right atrial appendages obtained from patients at the time of heart surgery. Arterioles were cannulated and pressurized (70 mmHg), and changes in diameter were measured with a video caliper (Colorado).

Intraluminal flow was induced by changing perfusion pressure with equal degree but in opposite direction, in three steps (ΔP: 25–50–90 cmH_2O). Fig. 1*A* shows that ΔP elicited increases in flow (~8 to ~35 μL/min), which resulted in increases in WSS (from ~5 to ~15 dyne/cm^2). To assess the role of NO, $ONOO^-$, and NOS cofactor, tetrahydrobiopterin (BH_4) in affecting coronary FMD, coronary arterioles were incubated with NOS inhibitor, Nω-nitro-L-arginine methyl ester (L-NAME, 2×10^{-4} mol/L for 30 min), selective $ONOO^-$ sequesters, iron(III)tetrakis(*N*-methyl-4'pyridyl)porphyrin-pentachloride (FeTMPyP, 10^{-4} mol/L) and uric acid (10^{-4} mol/L for 30 min), or stable BH_4 precursor, sepiapterin (10^{-5} mol/L for 30 min), respectively, and coronary FMD was reassessed. In other protocols, after incubation with FeTMPyP or sepiapterin, vessels were exposed to additional L-NAME, and coronary FMD was obtained again. In separate protocols, arterioles were exposed to exogenous $ONOO^-$ (10^{-5} mol/L) and FMD was assessed. To investigate the role of caveolae, arterioles were preincubated with methyl-β-cyclodextrin (mβCD, 2×10^{-3} mol/L for 60 min), which is known to disrupt caveolae (20).

Detection of Superoxide Anion Production

Superoxide production in coronary arteries was measured by using the dihydroethidium (DHE) method, as described previously (10,11). In brief, cryosections (8-μm thick) from snap-frozen human atrium were incubated with DHE (10 μmol/L for 30 min) with or without pretreatment with superoxide scavenger Tiron (5 mmol/L for 30 min). Slides were washed in PBS, and sections were covered with DAPI-Vectashield. Fluorescence intensity measurements (excitation BP545/25; emission BP605/70) of oxidized, nuclei-trapped DHE were performed in nuclei in the vessel wall and normalized to nuclei area.

Immunohistochemistry and Proximity Ligation Assay for Colocalization

Atrial appendages from non-DM and DM patients were fixed in 4% paraformaldehyde and paraffin embedded.

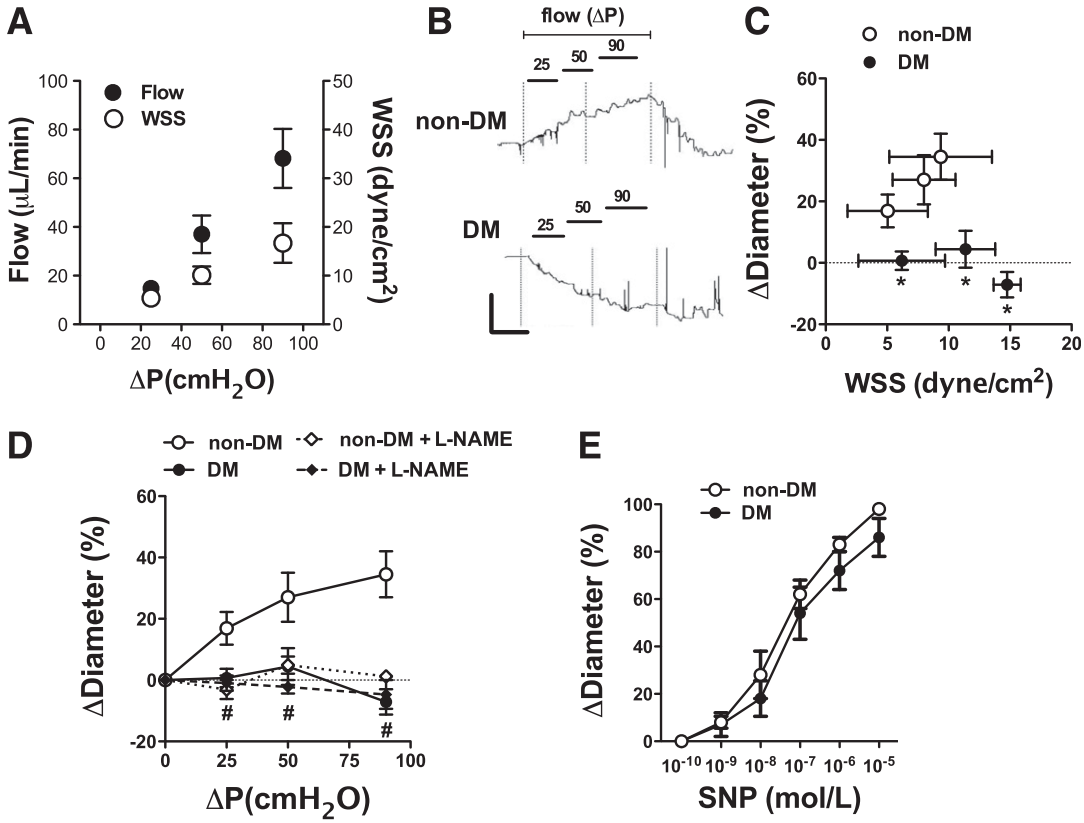

Figure 1—*A*: Step increases in inflow and outflow pressure (ΔP, 25, 50, and 90 cmH_2O) elicited increases in intraluminal flow (●) and resulted in increases in WSS (○). Representative recordings (*B*) and summary data of changes (*C*) in the diameter of coronary arterioles isolated from patients without (○, $n = 13$) and with DM (●, $n = 16$) in response to increases in WSS. *D*: WSS-induced changes in diameter of coronary arterioles of DM (●, $n = 4$) and non-DM patients (○, $n = 5$) in the absence and presence of the NOS inhibitor L-NAME (◇ and ◆, respectively). *E*: Changes in the diameter of coronary arterioles isolated from non-DM (○, $n = 7$) and DM (●, $n = 7$) subjects in response to NO donor, sodium nitroprusside (SNP). Data are means ± SEM. *, DM vs. non-DM patients; #, non-DM vs. non-DM+L-NAME. $P < 0.05$.

Consecutive sections (8-μm thick) were blocked with normal donkey serum (1 h) and immune labeled with monoclonal anti–caveolin 1 (Cav-1) (1:100, overnight 4°C; Abcam) and polyclonal anti–3-NT (1:1,000, overnight 4°C; Sigma-Aldrich) antibodies. Immunofluorescent labeling was performed with corresponding Cy3 and Cy5 secondary antibodies (Jackson ImmunoResearch). DAPI was used for nuclear staining. For nonspecific binding, the primary antibody was omitted. Images were collected with fluorescent microscopy. The colocalization between Cav-1 and 3-NT was calculated with linear regression and Pearson correlation coefficient (r), as described by Zinchuk et al. (21), in DM and non-DM patients by an investigator unaware of sample identity.

In additional experiments, in situ proximity ligation assay (PLA; Duolink; Sigma-Aldrich) was performed to detect colocalization of Cav-1 and 3-NT according to manufacturer instructions. In brief, PLA reactions were performed using the same primary antibodies (anti–Cav-1 [1:100] and anti–3-NT [1:1,000]), followed by a pair of oligonucleotide-labeled secondary antibodies (orange PLA probes). In this assay, PLA probes create a positive signal only when the epitopes of the target proteins are in close proximity (<40 nm). The signal from each detected pair of PLA probes was then counted using fluorescence microscopy (excitation BP545/25; emission BP605/70). For negative controls, primary antibodies were omitted.

Immunoelectron Microscopy

Immunogold Labeling for 3-NT

The right atrial appendages were fixed in 4% formaldehyde and 0.2% glutaraldehyde in 0.1 mol/L sodium cacodylate buffer (pH 7.4). Sections were cut with Leica EM UC6 ultramicrotome (Leica Microsystems, Inc., Bannockburn, IL). Sections were blocked in normal goat serum (1 h) and incubated with primary rabbit anti–3-NT polyclonal antibody (1:10, overnight 4°C; Sigma-Aldrich) or anti–Cav-1 polyclonal antibody (1:100, overnight 4°C; Cell Signaling) and with additional gold-labeled (10 nm) secondary antibody. Sections were observed in a JEM 1230 transmission electron microscope (JEOL USA, Inc.). Counting of anti–3-NT-immunogold and anti–Cav-1-immunogold particles within coronary endothelial cells was evaluated by an investigator unaware of sample identity.

Assessment of Caveolae Number in Coronary Endothelial Cells

Electron microscopy of atrial samples was performed as described above. Images selected for analysis contained at least one erythrocyte to ensure accuracy in identifying the endothelial cell layer. The number of caveolae per μm^2 of cell membrane was counted, as described previously (22), and compared in DM and non-DM patients by an investigator unaware of sample identity. In separate protocols, atrial samples were exposed to increasing concentrations of exogenous $ONOO^-$ (1, 10, and 100 μmol/L), and the number of endothelial caveolae was calculated.

Western Immunoblot

Western immunoblot analysis was performed as described previously (5). In brief, coronary arterioles were homogenized in radioimmunoprecipitation assay buffer, and protein concentration was measured by Bradford assay. Equal amounts of proteins were loaded for gel electrophoresis. After blotting, a polyclonal anti–3-NT antibody (dilution 1:1,000) was used for the detection of 3-NT. Membranes were reprobed with anti–β-actin IgG (dilution 1:5,000) to normalize for loading variations. Corresponding horseradish peroxidase–labeled secondary antibody was used, and chemiluminescence was visualized autoradiographically.

Membrane Fractionation of Cultured Human Coronary Artery Endothelial Cells

Human coronary artery endothelial cells (HCAECs) (Lonza, Walkersville, CA) were grown in EBM-2 medium. Cells were maintained in normal (5.5 mmol/L) or high glucose medium (HG; 25 mmol/L for 24 h). HCAECs were then harvested for cell fractionation using ultracentrifugation. In brief, cells were washed in PBS and lysed in MSE extraction buffer (10 mmol/L Tris-HCl, 220 mmol/L D-mannitol, 70.1 mmol/L sucrose, 1 mmol/L EGTA, 0.025% BSA). Protein was measured (Bio-Rad), and equal amount of protein was centrifuged at 100,000*g* for 20 min. Supernatant was collected as cytosolic fraction, and pellet contained the membrane fraction. Equal amounts of total lysate and cytosolic and membrane fractions were loaded for Western blot analysis.

Assessment of Endothelium-Dependent Dilation in Cav-1 Knockout Mice

Protocols involving mice were approved by the Institutional Animal Care and Use Committee. Video microscopy and wire myography to assess coronary FMD (10,11) and relaxation of aorta were performed as described previously (23). In brief, the heart and thoracic aorta were excised from Cav-1 knockout (CavKo) (Cavtm1Mls/J; The Jackson Laboratory) and wild-type mice. Mouse coronary arteries (diameter ~100 μm) were isolated and pressurized (70 mmHg). Arteries were preconstricted with thromboxane analog, U46619 (10^{-9} mol/L). Diameter changes of arterioles to increases in WSS and ACh (10^{-9} to 10^{-6} mol/L) were measured with video microscopy. Aorta sections (2 mm in length) were mounted on wire myograph to measure isometric force generation. Aorta were preconstricted with phenylephrine (10^{-6} mol/L), and relaxation was assessed in response to ACh (10^{-9} to 10^{-6} mol/L). Coronary arteries and aortic rings were incubated with sepiapterin (10^{-5} mol/L, 30 min) or sepiapterin plus L-NAME (2×10^{-4} mol/L, 30 min), and WSS- and ACh-induced responses were reassessed.

Data Analysis

Statistical analyses were performed using IBM SPSS Statistics 19. Agonist-induced arteriole responses were expressed as changes in diameter as a percentage of the maximal dilation, defined as passive diameter of the vessel at 70 mmHg in calcium-free physiological salt solution. Aortic relaxations in mice were presented as percent changes in force after agonist administration. Statistical analysis was performed by repeated-measures ANOVA, followed by Tukey post hoc test. $P < 0.05$ was considered statistically significant. Data are expressed as mean ± SEM.

RESULTS

Patients

Patient demographics and clinical data are presented in Table 1. The age, sex, clinical parameters, underlying diseases, and medications were similar between the two populations, except the documented DM, glucose levels, and the use of insulin or oral antidiabetics. Patients with DM were more likely to undergo coronary artery bypass graft surgery than non-DM patients. Thus, the potential influence of antidiabetic medications and the type of the surgery on the measured end points cannot be entirely excluded in this study.

NO-Dependent FMD Is Diminished in Coronary Arterioles of DM Patients

In isolated coronary arterioles, a spontaneous tone developed in response to 70 mmHg intraluminal pressure. There were no significant differences between the active (non-DM, 105 ± 7 μm; DM, 94 ± 7 μm) and passive (non-DM, 143 ± 8 μm; DM, 123 ± 7 μm) diameters in DM and non-DM patients. Incubation with sepiapterin, $ONOO^-$ sequesters, FeTMPyP, uric acid, and/or L-NAME had no effect on the spontaneously developed tone (data not shown).

In coronary arterioles of non-DM patients, increases in intraluminal flow, via increasing WSS (Fig. 1*A*), elicited dilations, whereas coronary arterioles from DM patients exhibited a diminished FMD (Fig. 1*B* and *C*). The NOS inhibitor L-NAME reduced coronary FMD in non-DM, but not in DM, patients (Fig. 1*D*). Dilations to the NO donor sodium-nitroprusside were similar in DM and non-DM patients (Fig. 1*E*).

Table 1—Patient demographics, diseases, and medications

	Non-DM	DM	*P*
n	37	41	
Male	26	29	1.000
Age (years)	65 ± 15	69 ± 10	0.180
Body weight (kg)	83 ± 25	89 ± 18	0.282
BMI (kg/m^2)	28.8 ± 7.4	31.1 ± 6.1	0.135
Systolic blood pressure (mmHg)	135 ± 25	136 ± 26	0.944
Diastolic blood pressure (mmHg)	73 ± 12	71 ± 12	0.492
Serum glucose (mg/dL)	115 ± 35	157 ± 71	0.004*
Underlying disease (*n*)			
Type 1 DM	0	2	0.494
Type 2 DM	0	39	<0.0001*
Hypertension	26	35	0.189
Hyperlipidemia	15	21	0.498
Coronary artery disease	23	30	0.474
Peripheral vascular disease	2	5	0.438
Congestive heart failure	9	5	0.237
Medications (*n*)			
Aspirin	25	31	0.807
Lipid lowering	20	25	0.655
Insulin	0	14	<0.0001*
Oral antidiabetic	0	27	<0.0001*
β-Blocker	23	29	0.636
ACE inhibitor	11	15	0.636
Diuretic	10	16	0.344
Anticoagulant	8	14	0.317
Calcium channel blocker	8	10	1.000
Surgical procedure (%)			
Coronary artery bypass graft	29	40	0.039*
Valve replacement	8	4	0.209

For continuous variables, mean ± SD are shown. All categorical risk factors were examined by Fisher exact tests, whereas continuous variables were assessed by Student *t* test between the two patient groups. *n*, number of non-DM and DM patients studied. *Statistical difference.

$ONOO^-$ Contributes to the Diminished Coronary Arteriolar FMD

We found a significantly increased DHE-detected, Tiron-inhibited superoxide production in coronary arteries of DM patients, when compared with non-DM (Fig. 2*A* and *B*). Moreover, the increased level of 3-NT in coronary arterioles indicated an augmented $ONOO^-$ production in DM patients (Fig. 2*C*). Incubation of coronary arterioles with the selective $ONOO^-$ scavengers FeTMPyP (Fig. 2*D*) or uric acid (Fig. 2*E*) significantly enhanced coronary FMD in DM, whereas exogenous application of $ONOO^-$ reduced coronary dilation in non-DM patients (Fig. 2*F*).

$ONOO^-$ Targets Endothelial Caveolae in DM

The subcellular localization of 3-NT was investigated in coronary arterioles using immune electron microscopy and immunohistochemistry approaches. Whereas 3-NT immunogold labeling was less prominent within the endothelium of non-DM patients, in DM, the number of 3-NT immunogold particles was increased and more widely distributed, with a significantly increased presence in the luminal plasma membrane of endothelium (Fig. 3*A* and Table 2 for detailed quantification).

To test whether $ONOO^-$ targets endothelial membrane caveolae, coimmunostaining of 3-NT and Cav-1 was performed. In coronary endothelial cells, a greater degree of colocalization between 3-NT and Cav-1 was found in DM patients, as indicated by Pearson correlations of fluorescence intensities (Fig. 3*B* and *C*). Colocalization of 3-NT and Cav-1 was confirmed by in situ PLA in further independent experiments (Fig. 3*D* and *E*).

Membrane-Localized Cav-1 Is Reduced in Coronary Endothelium of DM Patients

We found no significant change in total Cav-1 expression between coronary arteries of DM and non-DM patients (Fig. 4*A*). When distribution of Cav-1 immunogold particles was investigated by electron microscopy, we found that membrane-localized Cav-1 was significantly reduced in DM endothelium (Fig. 4 and Table 2). To confirm

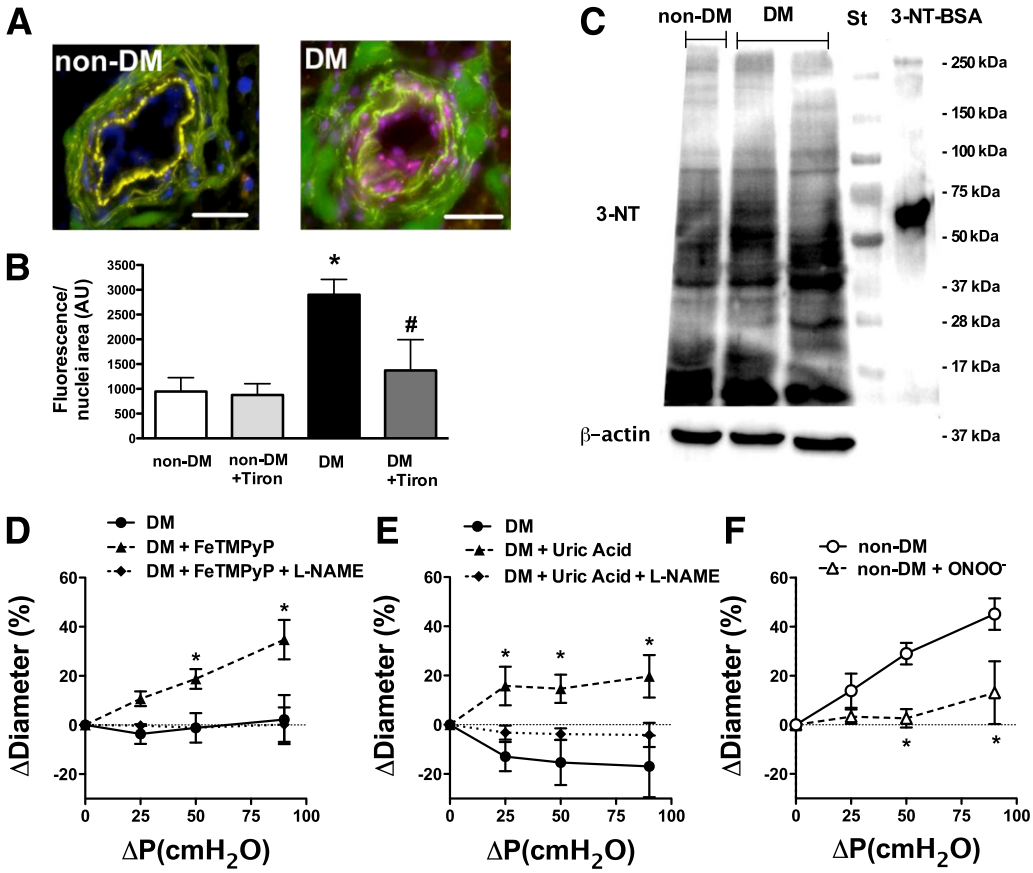

Figure 2—Representative fluorescent images of DHE staining (*A*) and summary data of fluorescent intensities/nuclei area (arbitrary unit [AU]) (*B*) in coronary arteries of non-DM ($n = 4$) and DM patients ($n = 3$). DAPI, blue; DHE fluorescence, red; autofluorescence, green (at 488 nm). Purple color indicates overlap of blue nuclei and strong DHE red fluorescence. Scale bar, 50 μm. *, DM vs. non-DM patients; #, DM vs. DM+Tiron. $P < 0.05$. *C*: Representative Western immunoblot shows 3-NT formation in coronary arterioles of non-DM and DM patients. St, molecular weight standard. 3-NT-BSA was used for positive control and anti–β-actin was used for loading variations. *D* and *E*: WSS-induced changes in diameter of coronary arterioles from patients with DM (●, $n = 5$) in the presence of $ONOO^-$ scavengers, FeTMPyP ($n = 5$) (*D*) or uric acid (▲, $n = 5$) (*E*) and also in the simultaneous presence of FeTMPyP or uric acid and L-NAME (◆, $n = 4$). *F*: WSS-induced changes in the diameter of coronary arterioles from non-DM patients (○, $n = 5$) after bolus exposure to exogenous $ONOO^-$ (10 μmol/L, △, $n = 4$). Data are means ± SEM. *, significant effects of various treatments. $P < 0.05$.

these changes in the membrane Cav-1 content, we also used primary cultured HCAECs that were exposed to high glucose (25 mmol/L) concentrations. We found that exposure of HCAECs to high glucose significantly reduced membrane Cav-1 content, whereas it did not alter total and cytosolic level of Cav-1 (Fig. 4*C* and *D*).

$ONOO^-$ Reduces the Number of Endothelial Caveolae

Electron microscopy was used to evaluate the number of endothelial caveolae in DM and non-DM patients (Fig. 5*A*). We found a significantly reduced number of endothelial caveolae in DM patients, when compared with non-DM (Fig. 5*B* and *C*). Moreover, coronary arteries were exposed to exogenous $ONOO^-$. $ONOO^-$, in a dose-dependent manner reduced the number of endothelial caveolae (Fig. 5*D* and *E*). $ONOO^-$, at the highest concentration, disrupted the integrity of the endothelial membrane, which was lacking any caveolae and showed signs of membrane blebbing.

Lack of Caveolae Contributes to Endothelial NOS Uncoupling in DM

We found that administration of sepiapterin, a stable precursor of BH_4 significantly enhanced coronary FMD in DM patients, in an NO-dependent manner, while it did not affect dilation in non-DM patients (Fig. 6*A*). Pharmacologic disruption of caveolae with mβCD entirely abolished FMD in coronary arterioles in non-DM patients, which was partially restored by additional administration of sepiapterin (Fig. 6*B*).

To provide additional evidence for the lack of caveolae contributing to endothelial NOS (eNOS) uncoupling, CavKO mice were used. A phenotypic characteristic of CavKO mice is the complete lack of endothelial caveolae (24), which we also observed in this study (data not shown). We found that increases in WSS elicited dilations in wild-type mice but caused constrictions in coronary arteries of CavKO mice, which was converted to dilation by sepiapterin, in an NO-dependent manner (Fig. 6*C* and

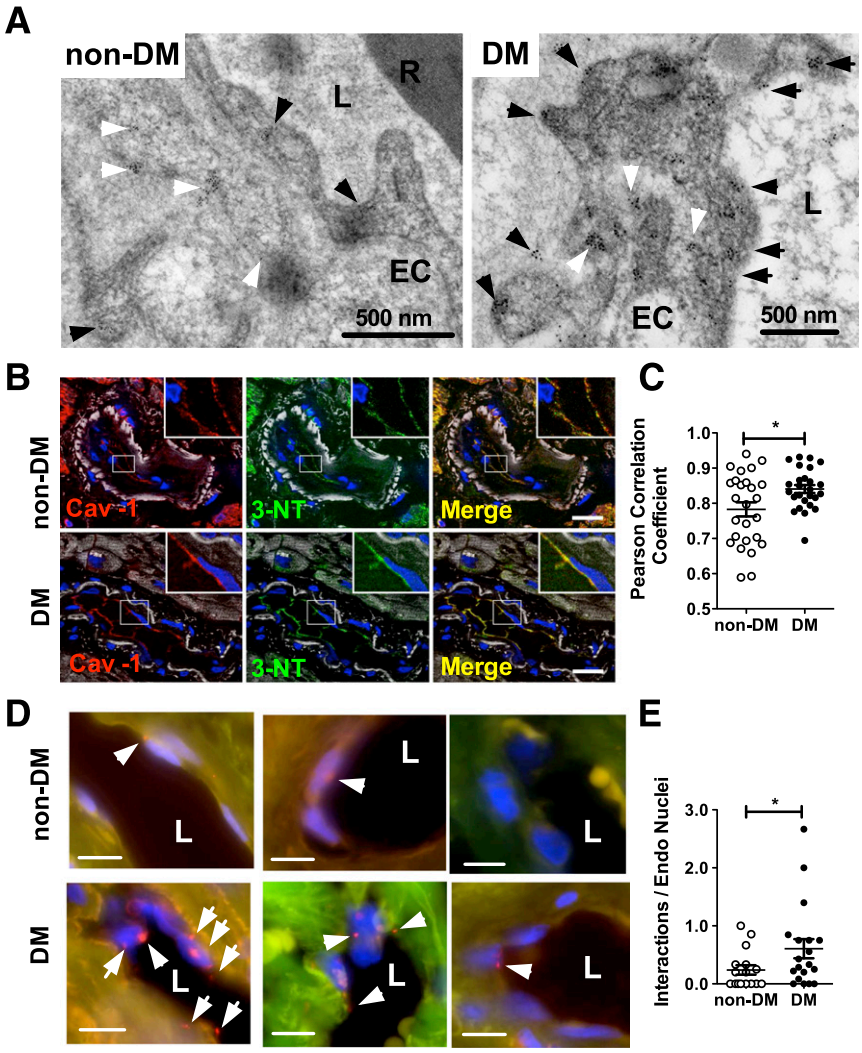

Figure 3—*A*: Electron micrograph illustration shows subcellular distribution of anti–3-NT immunogold particles (10 nm) in coronary arteriolar endothelium in non-DM (*left*) and DM patients (*right*). For detailed quantitative assessment of 3-NT nanogold distribution, see Table 2. Black arrowheads indicate 3-NT localization in close proximity to the luminal or abluminal plasma membrane, whereas white arrowheads point to cytosolic localization. EC, endothelium; L, vessel lumen; R, erythrocyte. *B*: Representative immunohistochemistry images for colocalization of Cav-1 and 3-NT in coronary arterioles of non-DM and DM patients. Blue, DAPI (nuclei); red, Cav-1; green, 3-NT; yellow, overlap of red and green signal; white, autofluorescence (at 488 nm). Scale bar, 20 μm. *C*: Summary data of Pearson correlation analysis for determining the degree of colocalization of Cav-1 and 3-NT. Random regions (26 and 26 from three non-DM and three DM patients) along endothelial cells were selected manually, and a scatterplot of Cav-1 and 3-NT fluorescent intensities (normalized to the background adjacent to the region of interest) was generated. ImageJ (NIH) was used to determine pixel signal intensities for each region of interest. *D*: Representative immunohistochemistry images of PLA for colocalization of Cav-1 and 3-NT in coronary endothelium of non-DM (*top panels*) and DM patients (*bottom panels*). *E*: Summary data represent PLA-positive signals obtained in five non-DM and seven DM patients. Three coronary vessels from each patient were analyzed for the number of PLA-positive interactions (shown as red blobs) around the endothelial (ENDO) nuclei (DAPI shown in blue). Green, autofluorescence (at 488 nm). White arrowheads point to PLA-positive signals. Scale bar, 15 μm. Data are means ± SEM. *, non-DM vs. DM patients. $P < 0.05$.

D). There was no difference in ACh-induced coronary dilation in wild-type and CavKO mice either in the absence or presence of sepiapterin, and the responses were only partially inhibited by L-NAME (Fig. 6*E*). In the aorta of CavKO mice, administration of sepiapterin significantly enhanced relaxation to ACh, and the response was abolished by additional L-NAME, suggesting a greater contribution of NO to ACh response in the mouse aorta (Fig. 6*F*).

DISCUSSION

This study demonstrates that in coronary resistance, arteries of diabetic patients increased production of $ONOO^-$ targets and disrupt endothelial caveolae, which in turn contributes to uncoupling of eNOS and results in a diminished FMD. This conclusion is supported by key findings. *1)* In coronary arterioles of DM patients, $ONOO^-$ sequester restored FMD, whereas in non-DM patients, exogenous $ONOO^-$ reduced FMD. *2)* 3-NT

Table 2—Quantification of 3-NT and Cav-1 immunogold distribution

	Non-DM	DM	*P*
3-NT nanogold			
Total in endothelium/μm^2	11.0 ± 1.4	42.4 ± 9.4	0.077
Luminal membrane/μm	1.2 ± 0.5	7.9 ± 1.4	0.029*
Abluminal membrane/μm	1.2 ± 0.5	3.6 ± 1.3	0.189
Cytosol/μm^2	8.6 ± 1.4	18.0 ± 5.5	0.223
Luminal/total (%)	12 ± 3	44 ± 6	0.016*
Cytosol/total (%)	77 ± 6	39 ± 5	0.007*
Cav-1 nanogold			
Total in endothelium/μm^2	19.7 ± 2.9	20.9 ± 4.9	0.852
Luminal membrane/μm	4.0 ± 0.4	2.0 ± 0.5	0.042*
Abluminal membrane/μm	1.6 ± 0.5	2.7 ± 0.6	0.217
Cytosol/μm^2	9.3 ± 1.8	13.4 ± 3.2	0.330
Luminal/total (%)	38 ± 4	15 ± 1	0.023*
Cytosol/total (%)	47 ± 2	64 ± 4	0.033*

Data are number of immunogold particles/endothelial surface area (μm^2) or number of particles on membrane/length (μm). In the case of 3-NT immunogold labeling, a total of 117.5 μm (10 cells from four non-DM patients) and 127.5 μm (nine cells from four DM patients) membrane was analyzed. In the case of Cav-1 immunogold labeling, a total of 214.1 μm (11 cells from four non-DM patients) and 184.7 μm (12 cells from four DM patients) membrane was analyzed. Data are mean ± SEM. *Statistical difference, $P < 0.05$ (Student *t* test).

staining was localized at the endothelial plasma membrane in a close proximity to Cav-1. *3*) Coronary arterioles of DM patients exhibited a reduced level of membrane-localized Cav-1 and also a reduced number of endothelial caveolae. *4*) The BH_4 precursor sepiapterin enhanced coronary FMD after pharmacological or genetic (CavKO mice) disruption of caveolae. Finally, *5*) sepiapterin restored coronary FMD in DM patients.

A solid line of evidence indicates that increased production of $ONOO^-$ plays an important role in the development of cardiovascular complications in DM (15). $ONOO^-$ is a powerful oxidizing agent that causes rapid depletion of sulfhydryl groups, causes DNA damage and protein nitration of aromatic amino acid residues leading to 3-NT formation (15). Cellular mechanisms to prevent the deleterious effect of $ONOO^-$ are not clearly defined (25). Previous studies have shown a significantly enhanced formation of 3-NT in the coronary endothelium in sepsis (26), in the coronary artery wall in human transplant coronary artery disease (27), and in coronary vessels in an animal model of DM (28). In this study, we found an elevated superoxide anion and increased 3-NT formation in coronary microvessels of DM patients. Given that the two patient populations exhibited similar comorbidities, it is likely that among various confounding factors, DM and most likely high blood glucose concentration are the major contributors for enhanced $ONOO^-$ formation in patients undergoing heart surgery. Importantly, in this study, we found that $ONOO^-$, in a reversible manner, diminishes NO-dependent FMD in coronary arterioles of DM patients.

Next, we aimed to elucidate $ONOO^-$-targeted subcellular mechanisms that are responsible for diminished NO availability in coronary arterioles of DM patients. Under physiological conditions, $ONOO^-$ production, as detected by 3-NT, is restricted to the mitochondria of the vascular endothelium (16). WSS-dependent activation of eNOS, on the other hand, is primarily coupled to regulatory mechanisms at the endothelial plasma membrane, although some evidence indicates involvement of mitochondria in this process (29). Among others, platelet endothelial cell adhesion molecule-1 (30,31) and endothelial caveolae (18) located at the plasma membrane have been shown to mediate WSS-dependent vasodilation in rodents. Given that $ONOO^-$ causes lipid peroxidation (15), we wondered whether $ONOO^-$ preferentially targets and interferes with vasoregulatory mechanisms intrinsic to the endothelial plasma membrane. In this study, we found that 3-NT immunogold particles were more abundant in the plasma membrane of the coronary endothelium in DM patients. We also demonstrated that 3-NT staining was in close proximity (<40 nm) to Cav-1, the main scaffolding protein of caveolae. There are four tyrosine groups within Cav-1 that can be potentially nitrated. Whether 3-nitration of Cav-1 has any functional consequence is entirely unknown. To investigate possible effects of $ONOO^-$ and Cav-1 interaction in DM, we measured Cav-1 expression in coronary arteries and found no significant changes between DM and non-DM patients. Interestingly, immune electron microscopy has revealed that the membrane-localized Cav-1 is significantly reduced in the coronary endothelium of DM patients. The reduced level of membrane Cav-1 was also confirmed in cultured human coronary endothelial cells that were exposed to high glucose concentrations for 24 h. Based on these results, we raised the possibility that alterations in the membrane-localized Cav-1 content may influence the formation and/or stability of endothelial caveolae in DM. Indeed, in this study, we found that DM patients exhibited a significantly reduced number of coronary endothelial caveolae. We also demonstrated that short-term administration of exogenous $ONOO^-$ elicited a dose-dependent, significant caveolae loss. In line with this observation, an earlier study has shown that even a short-term myocardial ischemia, due to a temporary occlusion of the coronary artery in anesthetized dogs, elicited a significant loss of caveolae in coronary vessels (32). A later study by Peterson et al. (33) showed that bovine aortic endothelial cells acutely exposed to a superoxide-generating napthoquinolinedione resulted in loss of endothelial cell caveolae. Collectively, we propose that a reduced membrane-localized Cav-1 may lead to destabilization and/or disruption of endothelial caveolae in coronary arterioles of DM patients. We suggest that a direct interaction between $ONOO^-$ and Cav-1 is

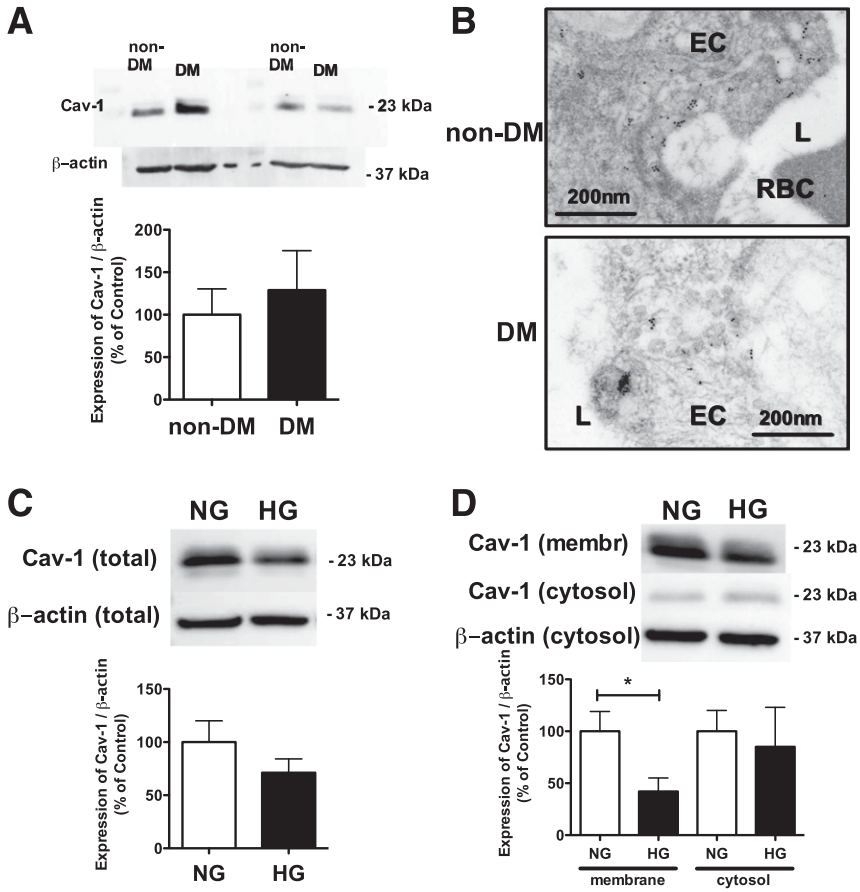

Figure 4—*A*: Representative Western immunoblot and summary data of densitometry analysis show Cav-1 expression in coronary arterioles of non-DM and DM patients (n = 6 non-DM and n = 6 DM). Anti–β-actin was used for normalizing loading variations. *B*: Electron micrograph illustration shows subcellular distribution of anti–Cav-1 immunogold particles (10 nm) in coronary arteriolar endothelium in non-DM (*top*) and DM (*bottom*) patients. For detailed quantitative assessment of Cav-1 nanogold distribution, see Table 2. EC, endothelium; L, vessel lumen; RBC, erythrocyte. Representative Western immunoblot and summary data of densitometry analysis of three independent experiments show Cav-1 expression in total lysate (*C*) or membrane and cytosole fractions (*D*) of HCAECs in the presence of normal glucose (NG; 5.5 mmol/L) or after HG (25 mmol/L) exposure. Anti–β-actin was used for normalizing loading variations. *, NG vs. HG. $P < 0.05$.

responsible for this pathology. Whether $ONOO^-$-induced 3-nitration of Cav-1 contributes to this process or only represents a "footprint" of Cav-1 targeting by $ONOO^-$ has yet to be elucidated.

How disruption of endothelial caveolae by $ONOO^-$ contributes to an impaired NO synthesis is not well understood. A study by Peterson et al. (34) demonstrated that Cav-1, eNOS, and GTPCH-I, the rate-limiting enzyme for BH_4 biosynthesis, are all localized in the endothelial caveolea. This and other studies indicated a crucial role for caveolae in the compartmentalization of enzymes that are required for NO synthesis (35). It is also known that the interaction between Cav-1 and eNOS is inhibitory (36–38). Loss of caveolae, through exposing endothelial cells to oxidized LDL, cyclosporine, or mβCD has been shown to displace eNOS from the plasma membrane, which is, however, associated with a diminished NO production (39–41). A study by Zhang et al. (42) showed that in endothelial cells, the plasma membrane–targeted eNOS was more efficient to produce NO when compared with the Golgi-targeted eNOS. Moreover, a recent elegant study demonstrated that a noninhibitory mutant of the Cav-1 scaffolding domain, without interfering with other functions of endogenous Cav-1, such as forming caveolae, significantly enhanced eNOS-derived NO synthesis (43). These studies indicated that under normal conditions, the interaction between Cav-1 and eNOS directs eNOS to the caveolae, and that this compartmentalization seems important for eNOS activation and NO production. Given that loss of caveolae structure/function may ultimately lead to an impaired NO synthesis. In order to furnish functional evidence for this scenario, in this study, human coronary arterioles were acutely treated with mβCD to disrupt vascular caveolae. We found that mβCD completely abolished NO-dependent coronary FMD in non-DM patients. Correspondingly, we found that increases in flow induced coronary arterial constrictions in CavKO

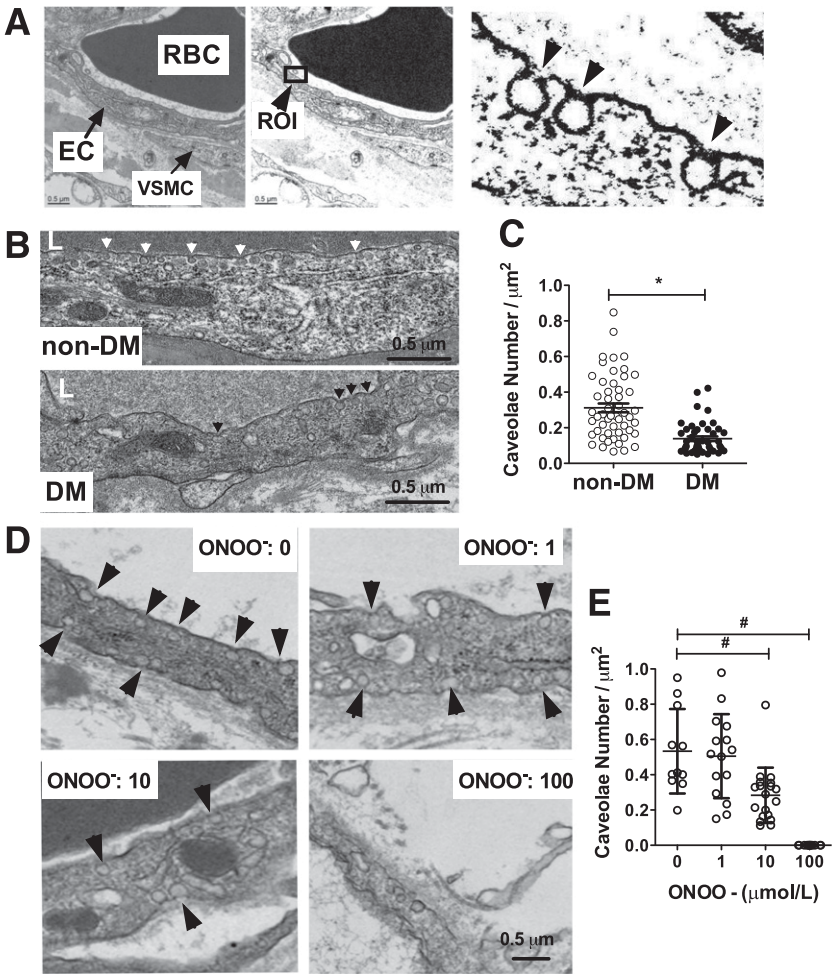

Figure 5—Electron microscopy for quantitative analysis of caveolae. *A*: Scheme for analysis of the electron microscopy images. Endothelial cells (ECs) were identified as those regions adjacent to erythrocytes (RBC). VSMC, vascular smooth muscle cell (*left*). A photo editor was used to establish a threshold gate to assist in identifying caveolae in multiple regions of interest (ROIs) (*middle*). Caveolae (black arrowheads) within endothelial cells were defined as apical or basal invaginations open to the surface, and membranes for analysis had to contain at least one caveolae (*right*). *B*: Representative electron micrograph illustration of the coronary endothelium in non-DM (*top*, white arrowheads point at caveolea) and DM patients (*bottom*, black arrowheads point at caveolea). Scale bar, 0.5 μm. *C*: Summary data show comparison of the number of endothelial membrane caveolae per μm^2 in non-DM (○, data are from 53 membrane regions from three patients) and DM patients (●, data are from 46 membrane regions from three patients). Electron micrograph illustration (*D*) and summary data (*E*) demonstrate the effects of increasing concentrations (1–100 μmol/L) of exogenous $ONOO^-$ on the number of coronary endothelial caveolae. Scale bar, 0.5 μm. Black arrows point at caveolae. Data are means ± SEM. *, non-DM vs. DM patients; #, significant effect of $ONOO^-$ treatment. $P < 0.05$.

mice. Our data are the first, to our knowledge, to provide evidence for the crucial role of caveolae in mediating WSS-induced dilation in human coronary arterioles.

The impaired flow-induced coronary dilation after caveolae disruption can be mediated by several mechanisms. Due to the observed close proximity of eNOS to GTPCH-I (34), we raised the possibility that the availability for eNOS cofactor BH_4 is limited after caveolae disruption, which ultimately leads to eNOS uncoupling in DM patients (44,45). Interestingly, in the CavKO mice, the ratio of BH_4 to BH_2 is reduced in the myocardium, which leads to eNOS uncoupling and may contribute to the cardiopulmonary phenotype of these mice (46). In this study, we demonstrated that in mβCD-treated vessels, the stable BH_4 precursor sepiapterin partially restored dilation to flow in human coronary arterioles. Moreover, in mice lacking caveolae, we found that after sepiapterin administration, flow-induced coronary dilation was restored to the control levels, whereas sepiapterin enhanced aortic relaxation. Importantly, the diminished FMD in coronary arterioles of DM patients was also augmented by sepiapterin administration. Collectively, these results are the first to demonstrate that impairment in flow-induced, NO-dependent coronary dilation in DM patients is due to eNOS uncoupling, which is likely mediated by $ONOO^-$-dependent disruption of endothelial caveolae. It should be noted that the influence of $ONOO^-$ on the function of eNOS might not

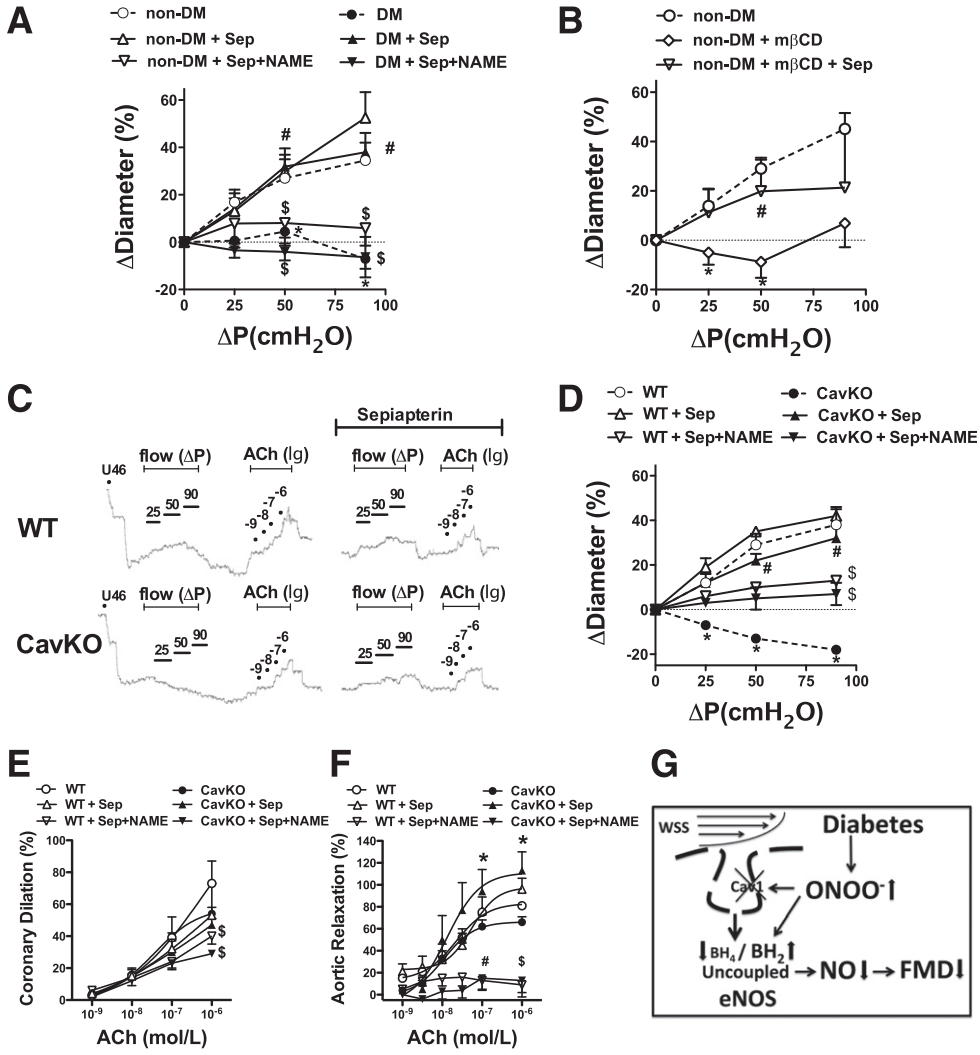

Figure 6—*A*: WSS-induced changes in diameter of coronary arterioles of non-DM (○ and dashed lines, $n = 5$) and DM patients (● and dashed lines, $n = 7$) before and after incubation with sepiapterin (Sep) (△ and ▲ in non-DM and DM, respectively), in the absence and presence of L-NAME (▽ and ▼ in non-DM and DM, respectively). *, non-DM vs. DM patients; #, DM vs. Sep; $, non-DM or DM vs. Sep+NAME. $P < 0.05$. *B*: WSS-induced changes in the diameter of coronary arterioles of non-DM patients (○ and dashed lines, $n = 6$) in the presence of mβCD (◇, $n = 4$) and in the simultaneous presence of mβCD and Sep (▽, $n = 4$). *, non-DM vs. mβCD; #, mβCD vs. mβCD+Sep. $P < 0.05$. Representative recordings (*C*) and summary data (*D*) of changes in the diameter of coronary arterioles isolated from wild-type (WT, ○, $n = 4$) or CavKO mice (●, $n = 4$) in response to increases in flow or increasing concentrations of ACh (10^{-9} to 10^{-6} mol/L) (*E*) in the absence and presence of Sep (△ and ▲ in WT and CavKO, respectively) or in the simultaneous presence of Sep plus L-NAME (▽ and ▼ in WT and CavKO, respectively). *, WT vs. CavKO; #, CavKO vs. Sep; $, WT or CavKO vs. Sep+NAME. $P < 0.05$. *F*: Percent changes in aortic relaxation in response to increasing concentration of ACh (10^{-9} to 10^{-6} mol/L) in WT (○, $n = 8$) and CavKO mice (●, $n = 8$), in the absence and presence of Sep (△ and ▲ in WT and CavKO, respectively) or in the simultaneous presence of Sep plus L-NAME (▽ and ▼ in WT and CavKO, respectively). *, CavKO vs. Sep; #, WT vs. Sep+NAME; $, CavKO vs. Sep+NAME. Data are means ± SEM. *G*: Schematic drawing illustrates the proposed novel mechanism by which $ONOO^-$ targets and disrupts coronary endothelial caveolae and that a disrupted caveolae predisposes eNOS cofactor BH_4 to $ONOO^-$ dependent oxidation, resulting in a diminished WSS-induced, NO-mediated coronary dilation in DM.

be limited to the disruption of coronary endothelial caveolae. It has been shown that $ONOO^-$ directly interacts and reduces the level of BH_4, as it has greater affinity for BH_4 than that of ascorbic acid and glutathione (47). Chen et al. (48) demonstrated that exposure of human eNOS to $ONOO^-$ resulted in a dose-dependent loss of activity with a marked destabilization of the eNOS dimer. They found that both free and eNOS-bound BH_4 were oxidized by $ONOO^-$; however, full oxidation of eNOS protein–bound BH_4 required significantly higher $ONOO^-$ concentrations (48). Based on the presented data, we also support the direct interaction between $ONOO^-$ and BH_4, which explains why $ONOO^-$ scavenger and sepiapterin fully restore coronary dilation in DM patients, in spite of having a reduced number of caveolae. Based on the results of this study, we propose a novel "upstream" mechanism by which $ONOO^-$ targets and disrupts coronary endothelial caveolae and that

a disrupted endothelial caveolae predisposes BH_4 to $ONOO^-$-dependent oxidation in DM (Fig. 6*G*). Restoring endothelial caveolae via $ONOO^-$ sequestration and/or treatment with a stable BH_4 precursor may facilitate NO production in the diseased coronary artery, a therapeutic strategy, which may prove beneficial to improve cardiovascular morbidity and mortality in DM.

Acknowledgments. The authors thank Robert Smith, Penny Roon, and Perry Libby (Electron Microscopy and Histology Core Laboratory, Georgia Regents University) for their assistance in the electron microscopy study.

Funding. This study was supported by Grant R01-HL-104126 from the National Heart, Lung, and Blood Institute (to Z.B.).

Duality of Interest. No potential conflicts of interest relevant to this article were reported.

Author Contributions. J.C. and Z.B. participated in the design of the study, performed experiments and the statistical analysis, and wrote the manuscript. H.D., I.C., A.S., and A.F. performed experiments. V.S.P., V.K., and E.B.d.C. participated in the design of the study and wrote the manuscript. M.J.R. participated in the design of the study, performed experiments, and wrote the manuscript. Z.B. is the guarantor of this work and, as such, had full access to all the data in the study and takes responsibility for the integrity of the data and the accuracy of the data analysis.

References

1. Mahgoub MA, Abd-Elfattah AS. Diabetes mellitus and cardiac function. Mol Cell Biochem 1998;180:59–64
2. Nitenberg A, Paycha F, Ledoux S, Sachs R, Attali JR, Valensi P. Coronary artery responses to physiological stimuli are improved by deferoxamine but not by L-arginine in non-insulin-dependent diabetic patients with angiographically normal coronary arteries and no other risk factors. Circulation 1998;97:736–743
3. Kaneda H, Taguchi J, Kuwada Y, et al. Coronary artery spasm and the polymorphisms of the endothelial nitric oxide synthase gene. Circ J 2006; 70:409–413
4. Miura H, Wachtel RE, Loberiza FR Jr, et al. Diabetes mellitus impairs vasodilation to hypoxia in human coronary arterioles: reduced activity of ATP-sensitive potassium channels. Circ Res 2003;92:151–158
5. Beleznai T, Feher A, Spielvogel D, Lansman SL, Bagi Z. Arginase 1 contributes to diminished coronary arteriolar dilation in patients with diabetes. Am J Physiol Heart Circ Physiol 2011;300:H777–H783
6. Koller A, Sun D, Kaley G. Role of shear stress and endothelial prostaglandins in flow- and viscosity-induced dilation of arterioles in vitro. Circ Res 1993;72:1276–1284
7. Camici PG, Crea F. Coronary microvascular dysfunction. N Engl J Med 2007;356:830–840
8. Lambert J, Aarsen M, Donker AJ, Stehouwer CD. Endothelium-dependent and -independent vasodilation of large arteries in normoalbuminuric insulin-dependent diabetes mellitus. Arterioscler Thromb Vasc Biol 1996; 16:705–711
9. Henry RM, Ferreira I, Kostense PJ, et al. Type 2 diabetes is associated with impaired endothelium-dependent, flow-mediated dilation, but impaired glucose metabolism is not; the Hoorn Study. Atherosclerosis 2004;174: 49–56
10. Bagi Z, Koller A, Kaley G. PPARgamma activation, by reducing oxidative stress, increases NO bioavailability in coronary arterioles of mice with type 2 diabetes. Am J Physiol Heart Circ Physiol 2004;286:H742–H748
11. Bagi Z, Koller A, Kaley G. Superoxide-NO interaction decreases flow- and agonist-induced dilations of coronary arterioles in type 2 diabetes mellitus. Am J Physiol Heart Circ Physiol 2003;285:H1404–H1410
12. Forstermann U, Sessa WC. Nitric oxide synthases: regulation and function. Eur Heart J 2012;33:829–837, 837a–837d
13. Forbes JM, Cooper ME. Mechanisms of diabetic complications. Physiol Rev 2013;93:137–188
14. Sharma A, Bernatchez PN, de Haan JB. Targeting endothelial dysfunction in vascular complications associated with diabetes. Int J Vasc Med 2012; 2012:750126
15. Pacher P, Beckman JS, Liaudet L. Nitric oxide and peroxynitrite in health and disease. Physiol Rev 2007;87:315–424
16. Heijnen HF, van Donselaar E, Slot JW, et al. Subcellular localization of tyrosine-nitrated proteins is dictated by reactive oxygen species generating enzymes and by proximity to nitric oxide synthase. Free Radic Biol Med 2006;40:1903–1913
17. van der Loo B, Labugger R, Skepper JN, et al. Enhanced peroxynitrite formation is associated with vascular aging. J Exp Med 2000;192:1731–1744
18. Yu J, Bergaya S, Murata T, et al. Direct evidence for the role of caveolin-1 and caveolae in mechanotransduction and remodeling of blood vessels. J Clin Invest 2006;116:1284–1291
19. Szerafin T, Erdei N, Fülöp T, et al. Increased cyclooxygenase-2 expression and prostaglandin-mediated dilation in coronary arterioles of patients with diabetes mellitus. Circ Res 2006;99:e12–e17
20. Feher A, Rutkai I, Beleznai T, et al. Caveolin-1 limits the contribution of BK(Ca) channel to EDHF-mediated arteriolar dilation: implications in diet-induced obesity. Cardiovasc Res 2010;87:732–739
21. Zinchuk V, Zinchuk O, Okada T. Quantitative colocalization analysis of multicolor confocal immunofluorescence microscopy images: pushing pixels to explore biological phenomena. Acta Histochem Cytochem 2007; 40:101–111
22. Sinha B, Köster D, Ruez R, et al. Cells respond to mechanical stress by rapid disassembly of caveolae. Cell 2011;144:402–413
23. Belin de Chantemèle EJ, Mintz JD, Rainey WE, Stepp DW. Impact of leptin-mediated sympatho-activation on cardiovascular function in obese mice. Hypertension 2011;58:271–279
24. Woodman SE, Ashton AW, Schubert W, et al. Caveolin-1 knockout mice show an impaired angiogenic response to exogenous stimuli. Am J Pathol 2003;162:2059–2068
25. Szabó C, Ischiropoulos H, Radi R. Peroxynitrite: biochemistry, pathophysiology and development of therapeutics. Nat Rev Drug Discov 2007;6:662–680
26. Kooy NW, Lewis SJ, Royall JA, Ye YZ, Kelly DR, Beckman JS. Extensive tyrosine nitration in human myocardial inflammation: evidence for the presence of peroxynitrite. Crit Care Med 1997;25:812–819
27. Ravalli S, Albala A, Ming M, et al. Inducible nitric oxide synthase expression in smooth muscle cells and macrophages of human transplant coronary artery disease. Circulation 1998;97:2338–2345
28. Li H, Gutterman DD, Rusch NJ, Bubolz A, Liu Y. Nitration and functional loss of voltage-gated K+ channels in rat coronary microvessels exposed to high glucose. Diabetes 2004;53:2436–2442
29. Liu Y, Zhao H, Li H, Kalyanaraman B, Nicolosi AC, Gutterman DD. Mitochondrial sources of H2O2 generation play a key role in flow-mediated dilation in human coronary resistance arteries. Circ Res 2003;93:573–580
30. Bagi Z, Frangos JA, Yeh JC, White CR, Kaley G, Koller A. PECAM-1 mediates NO-dependent dilation of arterioles to high temporal gradients of shear stress. Arterioscler Thromb Vasc Biol 2005;25:1590–1595

31. Liu Y, Bubolz AH, Shi Y, Newman PJ, Newman DK, Gutterman DD. Peroxynitrite reduces the endothelium-derived hyperpolarizing factor component of coronary flow-mediated dilation in PECAM-1-knockout mice. Am J Physiol Regul Integr Comp Physiol 2006;290:R57–R65
32. Kloner RA, Ganote CE, Jennings RB. The "no-reflow" phenomenon after temporary coronary occlusion in the dog. J Clin Invest 1974;54:1496–1508
33. Peterson TE, Poppa V, Ueba H, Wu A, Yan C, Berk BC. Opposing effects of reactive oxygen species and cholesterol on endothelial nitric oxide synthase and endothelial cell caveolae. Circ Res 1999;85:29–37
34. Peterson TE, d'Uscio LV, Cao S, Wang XL, Katusic ZS. Guanosine triphosphate cyclohydrolase I expression and enzymatic activity are present in caveolae of endothelial cells. Hypertension 2009;53:189–195
35. Cohen AW, Hnasko R, Schubert W, Lisanti MP. Role of caveolae and caveolins in health and disease. Physiol Rev 2004;84:1341–1379
36. García-Cardeña G, Martasek P, Masters BS, et al. Dissecting the interaction between nitric oxide synthase (NOS) and caveolin. Functional significance of the nos caveolin binding domain in vivo. J Biol Chem 1997;272:25437–25440
37. Michel JB, Feron O, Sacks D, Michel T. Reciprocal regulation of endothelial nitric-oxide synthase by Ca2+-calmodulin and caveolin. J Biol Chem 1997;272:15583–15586
38. Ju H, Zou R, Venema VJ, Venema RC. Direct interaction of endothelial nitric-oxide synthase and caveolin-1 inhibits synthase activity. J Biol Chem 1997;272:18522–18525
39. Lungu AO, Jin ZG, Yamawaki H, Tanimoto T, Wong C, Berk BC. Cyclosporin A inhibits flow-mediated activation of endothelial nitric-oxide synthase by altering cholesterol content in caveolae. J Biol Chem 2004;279:48794–48800
40. Blair A, Shaul PW, Yuhanna IS, Conrad PA, Smart EJ. Oxidized low density lipoprotein displaces endothelial nitric-oxide synthase (eNOS) from plasmalemmal caveolae and impairs eNOS activation. J Biol Chem 1999;274:32512–32519
41. Maniatis NA, Brovkovych V, Allen SE, et al. Novel mechanism of endothelial nitric oxide synthase activation mediated by caveolae internalization in endothelial cells. Circ Res 2006;99:870–877
42. Zhang Q, Church JE, Jagnandan D, Catravas JD, Sessa WC, Fulton D. Functional relevance of Golgi- and plasma membrane-localized endothelial NO synthase in reconstituted endothelial cells. Arterioscler Thromb Vasc Biol 2006;26:1015–1021
43. Bernatchez P, Sharma A, Bauer PM, Marin E, Sessa WC. A noninhibitory mutant of the caveolin-1 scaffolding domain enhances eNOS-derived NO synthesis and vasodilation in mice. J Clin Invest 2011;121:3747–3755
44. Vásquez-Vivar J, Martásek P, Whitsett J, Joseph J, Kalyanaraman B. The ratio between tetrahydrobiopterin and oxidized tetrahydrobiopterin analogues controls superoxide release from endothelial nitric oxide synthase: an EPR spin trapping study. Biochem J 2002;362:733–739
45. Alp NJ, Channon KM. Regulation of endothelial nitric oxide synthase by tetrahydrobiopterin in vascular disease. Arterioscler Thromb Vasc Biol 2004;24:413–420
46. Wunderlich C, Schober K, Schmeisser A, et al. The adverse cardiopulmonary phenotype of caveolin-1 deficient mice is mediated by a dysfunctional endothelium. J Mol Cell Cardiol 2008;44:938–947
47. Kuzkaya N, Weissmann N, Harrison DG, Dikalov S. Interactions of peroxynitrite, tetrahydrobiopterin, ascorbic acid, and thiols: implications for uncoupling endothelial nitric-oxide synthase. J Biol Chem 2003;278:22546–22554
48. Chen W, Druhan LJ, Chen CA, et al. Peroxynitrite induces destruction of the tetrahydrobiopterin and heme in endothelial nitric oxide synthase: transition from reversible to irreversible enzyme inhibition. Biochemistry 2010;49:3129–3137